Nuclear-localized CTP:phosphocholine cytidylyltransferase α regulates phosphatidylcholine synthesis required for lipid droplet biogenesis

Adam J. Aitchison, Daniel J. Arsenault, and Neale D. Ridgway
Departments of Pediatrics and of Biochemistry and Molecular Biology, Atlantic Research Centre, Dalhousie University, Halifax, NS B3H 4R2, Canada

ABSTRACT **The reversible association of CTP:phosphocholine cytidylyltransferase α (CCTα) with membranes regulates the synthesis of phosphatidylcholine (PC) by the CDP-choline (Kennedy) pathway. Based on results with insect CCT homologues, translocation of nuclear CCTα onto cytoplasmic lipid droplets (LDs) is proposed to stimulate the synthesis of PC that is required for LD biogenesis and triacylglycerol (TAG) storage. We examined whether this regulatory mechanism applied to LD biogenesis in mammalian cells. During 3T3-L1 and human preadipocyte differentiation, CCTα expression and PC synthesis was induced. In 3T3-L1 cells, CCTα translocated from the nucleoplasm to the nuclear envelope and cytosol but did not associate with LDs. The enzyme also remained in the nucleus during human adipocyte differentiation. RNAi silencing in 3T3-L1 cells showed that CCTα regulated LD size but did not affect TAG storage or adipogenesis. LD biogenesis in nonadipocyte cell lines treated with oleate also promoted CCTα translocation to the nuclear envelope and/or cytoplasm but not LDs. In rat intestinal epithelial cells, CCTα silencing increased LD size, but LD number and TAG deposition were decreased due to oleate-induced cytotoxicity. We conclude that CCTα increases PC synthesis for LD biogenesis by translocation to the nuclear envelope and not cytoplasmic LDs.**

Monitoring Editor
Howard Riezman
University of Geneva

Received: Mar 19, 2015
Revised: May 29, 2015
Accepted: Jun 16, 2015

INTRODUCTION

Major energy sources for eukaryotic cells are fatty acids, which are stored in a neutral esterified form as triacylglycerol (TAG) or cholesterol esters in cytoplasmic lipid droplets (LDs). The neutral lipid core of an LD is surrounded by a monolayer of phospholipids and associated proteins and enzymes that regulate stability and lipid metabolism (Pol *et al.*, 2014). The large uniocular LDs found in adipocytes are the main storage depots for neutral lipids, but other cells, including hepatocytes and macrophages, also have the capacity to store lipids in LDs. TAG stored in adipocyte LDs is hydrolyzed to release fatty acids during nutritional deficiency. Alternatively, the lipotoxic effects of circulating fatty acids are buffered by increased storage in LDs. Exceeding the lipid storage capacity of cells is linked to prevalent human diseases, including metabolic syndrome, hepatosteatosis, and atherosclerosis (Krahmer *et al.*, 2013).

LDs expand and contract, depending on the balance between synthesis and degradation of core neutral lipids. During LD expansion, surface phospholipids must be added coordinately with changes in core volume in order to maintain stability and prevent particle coalescence (Guo *et al.*, 2008). The phospholipid monolayer, which in mammalian cells contains 50–60% phosphatidylcholine (PC) and 20–30% phosphatidylethanolamine (PE), stabilizes the LD by decreasing surface tension and providing bending elasticity.

This article was published online ahead of print in MBoC in Press (http://www.molbiolcell.org/cgi/doi/10.1091/mbc.E15-03-0159) on June 24, 2015.

Address correspondence to: Neale D. Ridgway (nridgway@dal.ca).

Abbreviations used: BSA, bovine serum albumin; CCT, CTP:phosphocholine cytidylyltransferase; CEPT, choline/ethanolamine phosphotransferase; CPT, choline phosphotransferase; DAG, diacylglycerol; DPH, 1,6-diphenylhexatriene; ER, endoplasmic reticulum; FBS, fetal bovine serum; IEC, intestinal epithelial cell; LD, lipid droplet; LPCAT, lysophosphatidylcholine acyltransferase; PC, phosphatidylcholine; PE, phosphatidylethanolamine; PEMT, PE *N*-methyltransferase; PPAR, peroxisome proliferator-activated receptor; shRNA, short hairpin RNA; TAG, triacylglycerol; TLC, thin-layer chromatography.

In the early stages of LD biogenesis, phospholipids are acquired from the cytosolic leaflet of the endoplasmic reticulum (ER). However, the phospholipid composition and molecular species in cytosolic LDs are distinct from those of the bulk ER, indicating site-specific lipid synthesis, remodeling, or transport during LD maturation (Tauchi-Sato *et al.*, 2002; Bartz *et al.*, 2007). Depending on the cell type, PC on LDs is synthesized by PE *N*-methyltransferase (PEMT; Horl *et al.*, 2011), the Lands cycle enzymes lysophosphatidylcholine acyltransferases (LPCATs) 1 and 2 (Moessinger *et al.*, 2011), and de novo via the CDP-choline pathway (Krahmer *et al.*, 2011; Moessinger *et al.*, 2014). RNA interference (RNAi) silencing of PEMT in 3T3-L1 cells did not significantly affect PC mass but reduced TAG deposition by increasing lipolysis. Although PEMT has several transmembrane domains (Shields *et al.*, 2003), a GFP-tagged version was localized to the surface of LDs in 3T3-L1 cells (Horl *et al.*, 2011). Similarly, LPCAT1 or 2 synthesizes PC on isolated LDs when supplied with lyso-PC and acyl-CoA, and RNAi silencing of either enzyme in A431 cells reduced LD size and number as well as TAG mass (Moessinger *et al.*, 2011, 2014). Because the Lands cycle is a salvage and acyl-chain remodeling pathway, phenotypes related to LPCAT silencing could be a result of altered PC molecular species or lyso-PC accumulation. Nevertheless, Lands cycle and PEMT activity on the surface of LDs contributes directly to LD expansion and stability by provision of PC and/or consumption of lyso-PC or PE, respectively.

The CDP-choline pathway produces the majority of PC in mammalian cell membranes (Fagone and Jackowski, 2012) and is an important contributor to the phospholipid monolayer of LDs (Guo *et al.*, 2008). The pathway begins with choline uptake by high-, medium-, or low-affinity transporters, followed by ATP-dependent phosphorylation by cytosolic choline kinases. The synthesis of CDP-choline from phosphocholine and CTP is catalyzed by CTP:phosphocholine cytidylyltransferase α (CCTα), a ubiquitous nuclear enzyme (Cornell and Northwood, 2000), and CCTβ, a cytosolic enzyme with restricted tissue distribution (Lykidis *et al.*, 1998). Finally, choline/ethanolamine phosphotransferase (CEPT) and choline phosphotransferase (CPT) in the ER and Golgi apparatus, respectively, catalyze the synthesis of PC by transfer of phosphocholine from CDP-choline to diacylglycerol (DAG; Henneberry *et al.*, 2000, 2002). The rate of PC synthesis is controlled by CCTα, which alternates between a soluble, inactive form and a membrane-associated, active form. CCTα contains an α-helical domain M that preferentially interacts with membranes enriched in anionic lipids (e.g., fatty acids) or with lateral packing defects due to increased content of type II lipids (e.g., DAG and PE) and reduced PC (Yang *et al.*, 1995; Arnold and Cornell, 1996). Thus the membrane-sensing function of domain M allows CCTα to regulate PC synthesis in response to the relative proportion of pathway substrates and products. The nuclear/cytoplasmic distribution of CCTα also potentially regulates enzyme activity. By virtue of an N-terminal nuclear localization signal, CCTα is present in the nucleoplasm but translocates to the nuclear envelope, nucleoplasmic reticulum, and/or cytoplasm after stimulation with oleate or other lipophilic activators (Watkins and Kent, 1992; Lagace and Ridgway, 2005; Gehrig *et al.*, 2008b). In addition to lipid activators, other factors affect the nuclear–cytoplasmic distribution of CCTα, including its phosphorylation state, calcium, and proteolytic processing (Chen and Mallampalli, 2009; Agassandian *et al.*, 2010). The prevailing evidence suggests that CCTα cycles between the nucleus and cytoplasm and is selectively activated in either or both compartments, depending on the relative membrane content of PC and lipid activators.

The terminal enzymes in the CDP-choline pathway are not present on isolated LDs (Moessinger *et al.*, 2011). However, recent studies show that activation of the pathway is coupled to the biogenesis of cytosolic LDs by selective retention and activation of nuclear CCT on the surface of LDs. In *Drosophila* S2 cells treated with exogenous oleate, deletion of choline kinase, CCT1, or CCT2 increased LD size as a result of particle coalescence due to PC deficiency (Guo *et al.*, 2008; Krahmer *et al.*, 2011). mCherry-tagged CCT1, the insect homologue of mammalian CCTα, rapidly cycled between the nucleus and cytoplasm in untreated S2 cells and associated with the surface of expanding LDs that had reduced PC content or were enriched in lipid activators such as phosphatidic acid, DAG, and fatty acids. Increased localization and activity of CCT1 on the surface of LDs would provide the CDP-choline substrate for PC synthesis and incorporation into nascent LDs emerging from the ER. Alternatively, PC synthesized in the ER could be exported to LDs at contact zones (Kassan *et al.*, 2013).

A similar regulatory mechanism could occur in mammalian cells, since GFP-CCTα was partially localized on the surface of LDs and a fraction of endogenous CCTα was recovered in an isolated LD fraction from oleate-treated macrophages (Krahmer *et al.*, 2011). However, the model for CCT regulation of LD biogenesis was formulated using insect cells, in which PC is a minor component of LDs compared with PE. This naturally PC-deficient monolayer may not recapitulate the situation in mammalian cells, in which PC is more abundant. Indeed, our results using mammalian adipocyte and oleate-induced models of LD biogenesis indicate that activation of de novo PC synthesis regulates LD biogenesis by a mechanism that is independent to CCTα association with LDs.

RESULTS

CCTα expression and PC synthesis are induced during adipocyte differentiation

The differentiation of 3T3-L1 cells into adipocytes is accompanied by increased phospholipid synthesis and mass (Coleman *et al.*, 1978; Kasturi and Wakil, 1983). To assess whether the CDP-choline pathway contributed to increased PC synthesis, we monitored the expression of the initial and rate-limiting enzymes in the pathway by immunoblotting (Figure 1). During a 7-d differentiation period, 3T3-L1 cells showed a characteristic increase in peroxisome proliferator-activated receptor γ (PPARγ) and adiponectin expression (Figure 1A) and increased TAG mass, which reached a plateau at 5–7 d (Figure 1B). Coincident with the expression of these protein and lipid markers, CCTα protein expression gradually increased to a maximum of 15-fold relative to uninduced cells at days 5–7 (Figure 1C). The expression of the CCTβ isoform was not induced, nor was that of the initial enzyme in the pathway, choline kinase α.

The relationship between increased CCTα expression and flux through the CDP-choline pathway was assessed by metabolic labeling with [^{3}H]choline. At each day during the differentiation period, 3T3-L1 cells were incubated for 3 h in medium containing [^{3}H]choline, and isotope incorporation into PC, CDP-choline pathway intermediates (choline, phosphocholine, and CDP-choline), and the PC degradation product glycerophosphocholine was quantified (Figure 2). A significant increase in [^{3}H]choline incorporation into PC was observed at 3 d, followed by stabilization at days 4–7 at a level that was threefold increased relative to undifferentiated cells. [^{3}H]Choline incorporation into phosphocholine was reduced at days 3–7 but not significantly. Isotope incorporation into other metabolites, including the cellular [^{3}H]choline (unpublished data), was not affected during differentiation.

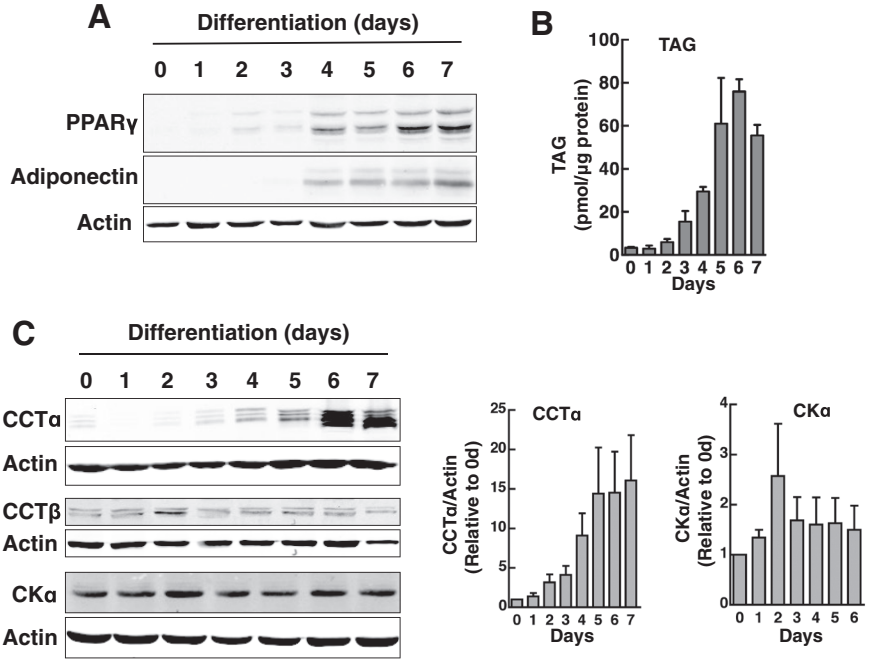

FIGURE 1: CCTα expression is induced during differentiation of 3T3-L1 preadipocytes. 3T3-L1 cells were differentiated over a 7-d period as described in *Materials and Methods*. (A, B) Expression of adipocyte differentiation markers PPARγ and adiponectin was monitored by immunoblotting of total cell lysates. Accumulation of cellular TAG mass was assayed using a colorimetric assay. (C) Total cell lysates of differentiating 3T3-L1 cells were immunoblotted for CCTα, CCTβ, and choline kinase α (CKα). CCTα and CKα expression was quantified relative to actin using a Li-Cor (Lincoln, NE) imaging system and normalized to values at day 0. Results are the mean and SD of three or four separate experiments.

Similar to results for 3T3-L1 cells, CCTα expression and PC synthesis were increased during differentiation of primary human preadipocytes (Figure 3). Human preadipocytes were differentiated over a 16-d period into TAG-laden adipocytes containing large LDs that occupied most of the cytoplasmic space (see later discussion of Figure 4B). Differentiation of human preadipocytes was accompanied by a twofold increase in CCTα protein expression at 12 and 16 d (Figure 3, A and B). The expression of CCTβ was unaffected during differentiation. Accompanying the increase in CCTα expression was an eight- to 10-fold increase in [^{3}H]choline incorporation into PC but not the water-soluble metabolites (Figure 3C).

CCTα localizes to the nucleus and nuclear envelop during adipocyte differentiation

Increased TAG synthesis in oleate-treated insect cells leads to export of nuclear, ectopically expressed CCTα onto the surface of LDs as a mechanism to coordinate expansion of the surface phospholipid monolayer and lipid core (Krahmer *et al.*, 2011; Payne *et al.*, 2014). To test whether this mode of regulation occurs during LD biogenesis in 3T3-L1 and human preadipocytes, we immunostained endogenous CCTα in conjunction with LD detection with BODIPY-493/503 (Figure 4). Before differentiation, CCTα was diffusely localized in the nucleoplasm of 3T3-L1 cells (Figure 4A). In cells that were differentiated for 2 d, CCTα was primarily in the nucleus but with evidence of weak cytoplasmic staining. With the appearance of LDs at 5 and 7 d, however, CCTα was more extensively localized to the nuclear envelope and the cytoplasm but was not detected on the surface of LDs (see expanded images on the right-hand side of Figure 4A). To rule out the possibility that CCTα might not be detected on cytoplasmic membranes or LDs by our C-terminal-specific antibody due to epitope masking, we used a commercial rabbit monoclonal antibody directed against an epitope in the N-terminus of CCTα. Similar to results shown in Figure 4A, the commercial monoclonal detected CCTα on the nuclear envelope and in the cytoplasm but not on LDs in differentiated 3T3-L1 cells (Supplemental Figure S1A). Thus results with two independently derived antibodies reveal that CCTα is activated on the nuclear envelope and/or cytoplasmic membranes. CCTα in human preadipocytes was also exclusively localized in the nucleus (Figure 4B). However, CCTα remained in the nucleus during differentiation and was not associated with the nuclear envelope or detected in the cytoplasm irrespective of the number or size of LDs in the adipocyte.

CCTα activity and PC synthesis regulate LD size

Induction of CCTα expression and PC synthesis during the differentiation of 3T3-L1 and human preadipocytes suggests that the CDP-choline pathway contributes PC for LD biogenesis. To test this, we transduced 3T3-L1 cells with lentivirus encoding a CCTα-specific short hairpin RNA (shCCTα) to achieve a >95% reduction in expression compared with cells expressing a control nontargeting short hairpin RNA (shNT; Figure 5A). CCTα silencing reduced PC synthesis (measured by [^{3}H] choline labeling) by 30 and 50% in 3T3-L1 cells at 0 and 7 d, respectively, effectively preventing the twofold increase in PC synthesis associated with differentiation (Figure 5B). Whereas CCTα silencing during differentiation of 3T3-L1 cells prevented the increase in PC synthesis, there was no effect on the expression of the differentiation-specific genes adiponectin (Figure 5, A and C) and PPARγ (Figure 5, A and D).

The 3T3-L1 cells in which CCTα was silenced for 7 d had fewer and larger BODIPY-493/503-stained LDs than did shNT controls (Figure 6A). Quantification of LD area revealed a significant reduction in small LDs (<2 μm) and an increase in large LDs (>20 μm) in differentiated cells transduced with lentiviral shCCTα versus shNT controls (Figure 6B). Accompanying this shift to toward larger LDs, CCTα silencing also caused a reduction in the total number of LDs (Figure 6C). TAG mass in CCTα-knockdown and control cells was similar regardless of the differentiation state (Figure 6D). Collectively this indicates that preventing the induction of PC synthesis by the CDP-choline pathway during 3T3-L1 differentiation affects LD size but does not compromise the ability of the adipocyte to store TAG.

CCTα localization and function during oleate-induced LD biogenesis

Most cultured cells take up and convert oleate into TAG for storage in cytoplasmic LDs that are structurally similar to those found in adipocytes. We tested whether CCTα and the CDP-choline pathway were regulated and/or required in this model of LD biogenesis. Initially, a number of cultured cell lines were treated with 400 μM oleate complexed to bovine serum albumin (BSA), and

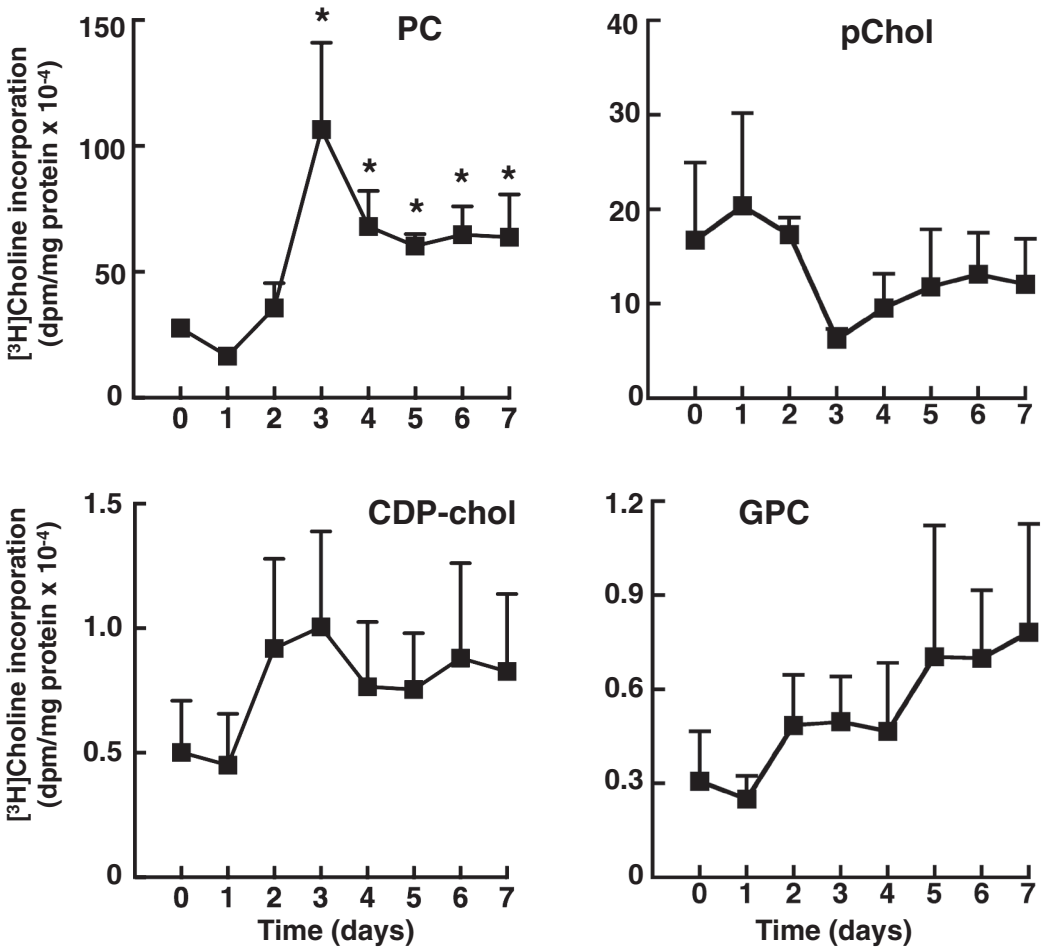

FIGURE 2: [^{3}H]choline incorporation into PC is stimulated during differentiation of 3T3-L1 preadipocytes. 3T3-L1 cells were differentiated over a 7-d period as described in *Materials and Methods*. At the indicated times, cells were pulse labeled with [^{3}H]choline (2 μCi/ml) for 3 h, and isotope incorporation into PC, phosphocholine (pChol), CDP-choline, and glycerophosphocholine (GPC) was measured. Results are the mean and SD of three experiments. *$p < 0.05$ compared to time 0 control.

LDs and CCTα were visualized by BODIPY-493/503 and immunostaining (Supplemental Figure S2, A–G). Treatment of CHO, HEK293, HeLa, HepG2, and 77A4, intestinal epithelial cell (IEC)-18, and IEC-ras4 cells with oleate/BSA for up to 24 h stimulated the formation of LDs of variable size and number. The most robust response was observed in IEC-18, ras-transformed IEC-18 (IEC-ras4), and HepG2 cells. Relocalization of nuclear CCTα during LD biogenesis was cell dependent: CHO, HEK293, IEC-ras4, and J77A4 cells displayed CCTα on the nuclear envelope; all cells had some degree of CCTα export to the cytoplasm; and cytoplasmic CCTα was diffuse or on punctate structures but not the surface of LDs. In IEC-ras4, CCTα was extensively localized to the nuclear envelope and cytoplasm after exposure to oleate for 24 h but did not associate with the surface of LDs (Supplemental Figure S2G).

The localization of epitope-tagged versions of CCTα was also visualized in live and fixed cells (Figure 7). Similar to results with the endogenous enzyme, CCT-GFP was primarily localized in the nucleus of CHO cells after oleate-treatment despite extensive cytoplasmic LD deposition (Figure 7A). CCT-mCherry was also localized in the nucleus of IEC-18 cells that contained cytoplasmic LDs (Figure 7A). Transiently expressed V5-tagged CCTα localized to the nucleoplasm or nuclear envelope of 12 h oleate-treated IEC-18 and IEC-ras4, respectively (Figure 7B). However, the steady-state distribution of epitope-tagged CCTα in the nucleoplasm and on the nuclear envelope does not rule out a dynamic, transient interaction with the cytoplasmic compartment. To test this, we subjected CHO cells expressing CCT-GFP and treated without and with oleate for 24 h to fluorescence loss in photobleaching (FLIP) analysis of the cytoplasmic and nuclear compartments (Figure 7, C and D). Fluorescence intensity in the nucleus of control and oleate-treated CHO cells declined by only 20% (compared with unbleached control nuclei) when regions of the cytoplasm, including those containing LDs, were subject to repeated photobleaching for 10 min (Figure 7C). Repeated photobleaching of a nuclear region resulted in a uniform and rapid >95% recline in total nuclear fluorescence (Figure 7E, oleate-treated CHO cell) that was delayed slightly in oleate-treated versus control CHO cells (Figure 7D). Of interest, residual nuclear envelope–associated CCT-GFP was observed at the end of the bleaching period in oleate-treated CHO cells but not in controls (Figure 7F). Exchange between the nuclear envelope and nucleoplasmic pool of CCT-GFP could explain the slight delay in photobleaching of the latter compartment in oleate-treated cells (Figure 7D).

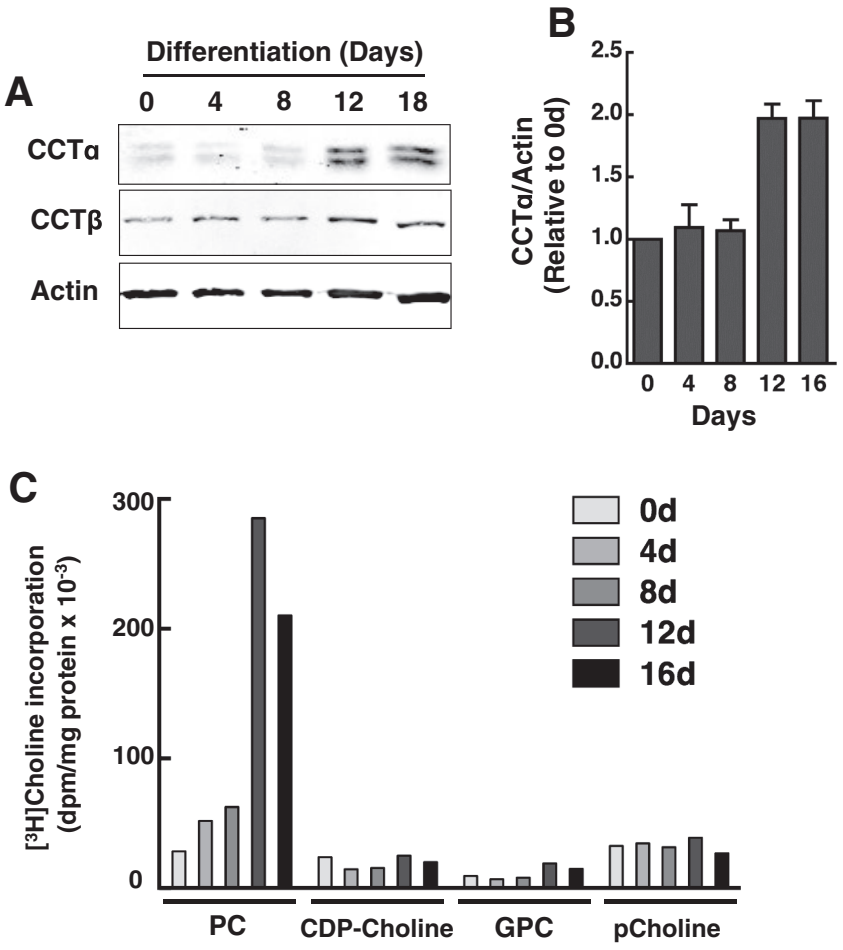

FIGURE 3: Induction of CCTα and PC synthesis during human preadipocyte differentiation. (A, B) At the indicated times during a 16-d differentiation period, total cell lysates of primary human adipocytes were collected and immunoblotted for CCTα and CCTβ. CCTα expression was quantified relative to actin using a Li-Cor imaging system and normalized to day 0. Results are the mean and SD of three separate experiments. (C) At the indicated times during differentiation, primary human adipocytes were pulse labeled with [^{3}H]choline (2 μCi/ml) for 3 h, and isotope incorporation into PC and water-soluble metabolites was measured. Results are the average of duplicate determinations from a representative experiment.

Similar to experiments with 3T3-L1 cells shown in Figure 6, we examined whether the CDP-choline pathway was required for LD formation in IEC-18 cells by silencing the expression of CCTα. IEC-18 stably transduced with lentiviral shCCTα had a >90% reduction in protein expression compared with shNT-expressing cells (Figure 8A). Treatment with 400 μM oleate/BSA for 24 h did not alter the expression of CCTα or the effectiveness of silencing. Control and CCTα knockdown IEC-18 cells were treated with oleate/BSA for 24 h, and the distribution of LDs was monitored by BODIPY-493/503 fluorescence. Reduction of CCTα expression in IEC-18 resulted in the appearance of larger LDs compared with shNT-expressing cells (Figure 8B). However, LD distribution in oleate-treated knockdown cells was heterogeneous, and these cells showed evidence of growth inhibition and shrinkage and had smaller nuclei than untreated counterparts and shNT controls. Quantitation of LD area confirmed that CCTα knockdown caused a significant increase in large LDs (>20 μm^2; Figure 8C), but the number of LDs/cell was reduced by 60% relative to oleate-treated shNT controls (Figure 8D). TAG mass in untreated shCCTα cells was increased approximately twofold compared with shNT cells, indicating that inhibition of PC synthesis diverted fatty acids into TAG (Figure 8E). However, treatment of shCCTα cells with oleate failed to stimulate TAG synthesis compared with controls. As mentioned, IEC-18 that express shCCTα appear to have a cytotoxic response to exogenous oleate that could be the result of reduced capacity to synthesize and store TAG. Using an 3-(4,5-dimethylthiazol-2-yl)-2,5diphenyltetrazolium bromide (MTT) assay to measure cell viability, it was apparent that control shNT cells were not significantly affected by exogenous oleate, but oleate concentrations >100 μM caused a significant reduction in the viability of IEC-18 in which CCTα was silenced (Figure 8F). Thus, compromising the CDP-choline pathway in IEC-18 increases LD size but also suppresses overall TAG storage in LDs, leading to excess unesterified oleate (or an oleate metabolite), which negatively affects cell viability.

DISCUSSION

The first and last reactions in the CDP-choline pathway take place in the cytoplasm and ER/Golgi apparatus, respectively, but the rate-limiting step catalyzed by CCTα occurs in the nucleus. Nuclear CCTα could contribute to PC synthesis by the transport of its substrates and product across the nuclear envelope. Alternatively, the enzyme is observed to translocate to the cytoplasm of cells that have an increased demand for PC. Under those conditions, cytosolic membranes that are PC deficient and/or enriched in lipid activators may recruit CCTα, leading to increased CDP-choline and PC synthesis. A similar regulatory scenario occurs during LD biogenesis in insect cells; CCT1 and CCT2 localize to the surface monolayer of LDs in response to PC deficiency and there produce CDP-choline required for PC synthesis and LD expansion (Guo *et al.*, 2008; Krahmer *et al.*, 2011). In this study, we show that PC synthesis by the CDP-choline pathway is required for expansion of cytoplasmic LDs in adipocytes and other mammalian cells, but the mechanism involves CCTα activation at the nuclear envelope.

Based on metabolic labeling and mass analysis, PC synthesis is found to increase during the differentiation of preadipocytes in culture. In 3T3-L1 cells, PC synthesis occurs by a concerted pathway involving increased phosphatidylserine synthesis and decarboxylation, followed by PE methylation to form PC (Horl *et al.*, 2011). We now show that the CDP-choline pathway, the major route for PC synthesis in mammalian cells, is also strongly induced during adipocyte differentiation. CCTα protein expression was increased 15-fold in 3T3-L1 cells after 5–7 d of differentiation, which coincided with a threefold increase in PC synthesis measured by [^{3}H]choline incorporation. The observed increase in CCTα protein expression is consistent with a report that CCTα mRNA was induced 30- to 40-fold during differentiation of 3T3-L1 cells (Kast *et al.*, 2001). PC made by the PE methylation and CDP-choline pathways could have different

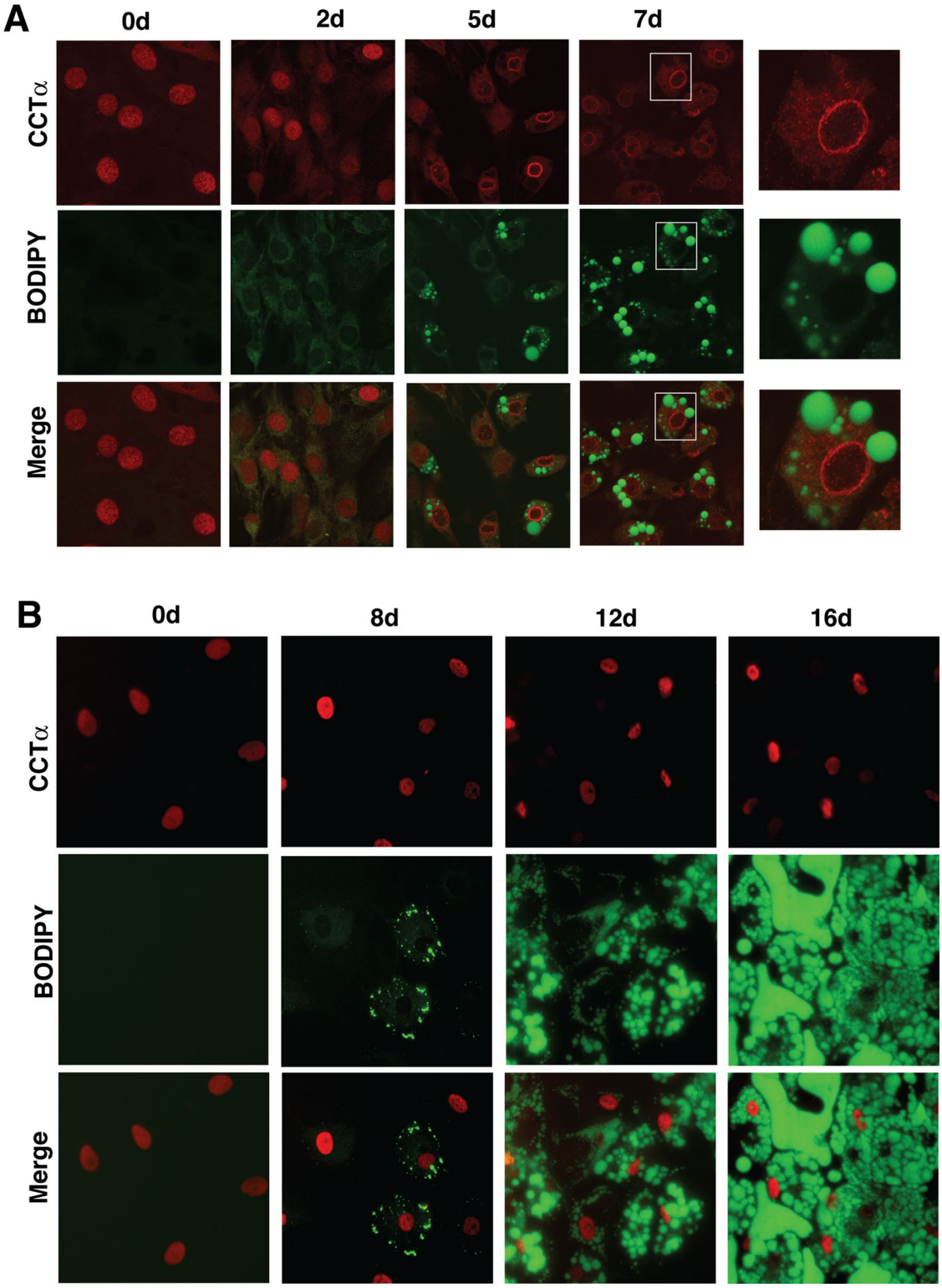

FIGURE 4: Nuclear CCTα does not associate with lipid droplets during 3T3-L1 or human preadipocyte differentiation. (A) At the indicated times during differentiation, 3T3-L1 cells were fixed, permeabilized, and immunostained with a CCTα primary antibody and an Alexa Fluor 594 secondary antibody. Lipid droplets were visualized with BODIPY-493/503. Right, enlarged images taken from the boxed areas for 7-d-differentiated cells. Images are 1-μm sections captured using a Zeiss LSM 510 META confocal microscope. Microscope settings for BODIPY imaging of 3T3-L1 cells were identical, but gain and pinhole settings for the 594-nm scan were adjusted due to increased CCTα overexpression at 5 and 7 d (Figure 1C). (B) Human preadipocytes differentiated over a 16-d period were fixed and immunostained for CCTα, and LDs were visualized with BODIPY-493/503 as described in A. Images are representative of three separate experiments.

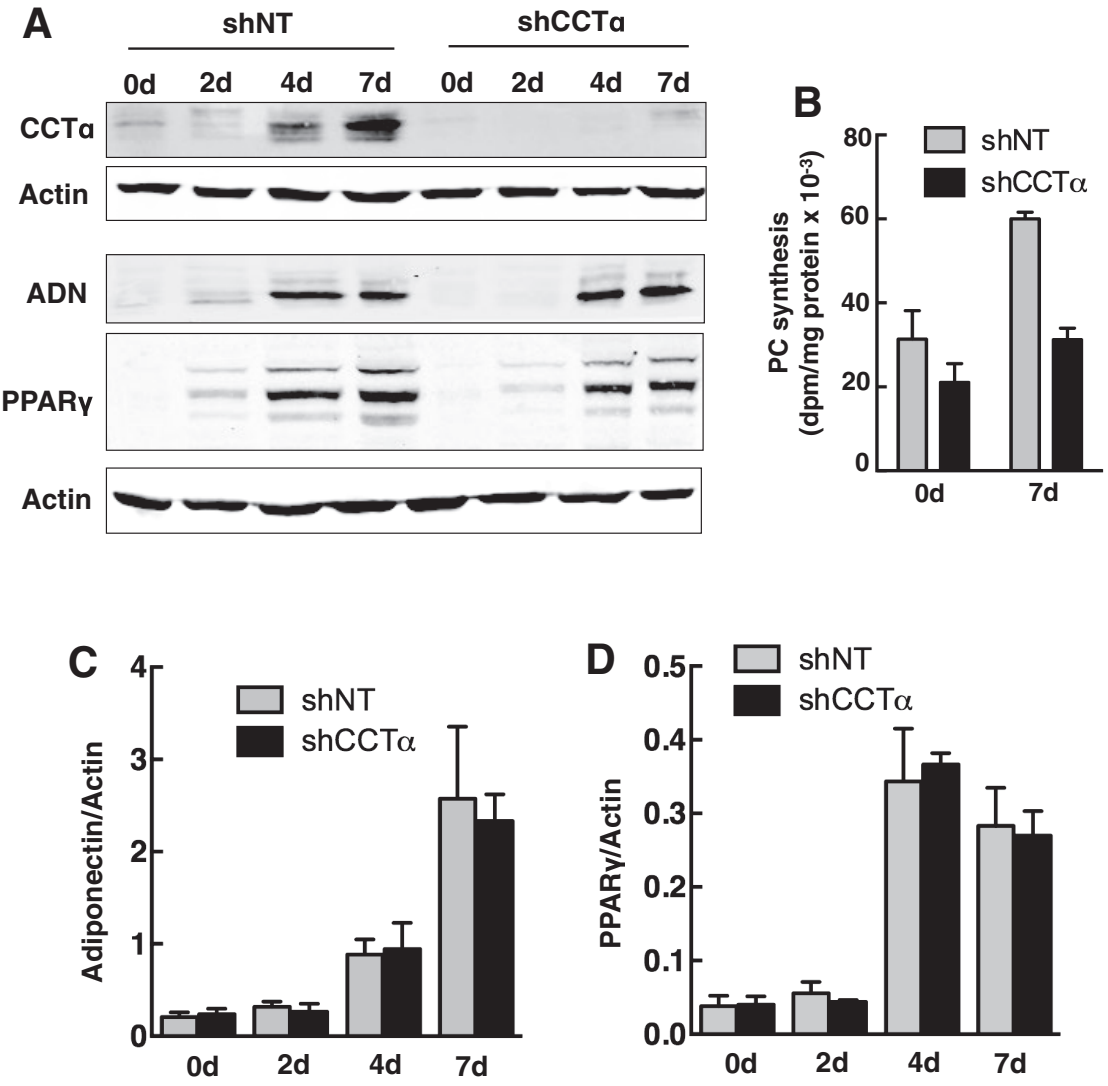

FIGURE 5: CCTα silencing does not affect the expression of 3T3-L1 cell differentiation markers. (A) 3T3-L1 preadipocytes were stably transduced with lentivirus encoding shCCT or shNT as described in *Materials and Methods*. CCTα knockdown and shNT control cells were incubated in differentiation medium, and at the indicated times total cell lysates were immunoblotted for CCTα, adiponectin (ADN), and PPARγ. (B) Undifferentiated (0 d) or 7-d-differentiated (7 d) 3T3-L1 cells expressing shNT or shCCTα were pulse labeled for 3 h with [^{3}H]choline (2 μCi/ml) to measure PC synthesis. Results are the mean and SD for three experiments. (C, D) Adiponectin and PPARγ expression in control shNT– and shCCTα-expressing 3T3-L1 cells during a 7-d differentiation period (shown in A) was quantified using a Li-Cor imaging system and normalized to actin expression. Results are the mean and SD of three separate experiments.

functions during adipocyte differentiation. Induction of the CDP-choline pathway would increase biosynthetic capacity from a source that already supplies the cell with the majority of its PC. In contrast, PEMT is virtually absent in preadipocytes and would supply PC with a unique molecular species composition (Ridgway and Vance, 1988) and in close proximity to the LD (Horl *et al.*, 2011). This may explain why silencing PEMT inhibited TAG accumulation in 3T3-L1 cells (Horl *et al.*, 2011), whereas we observed no effect on TAG mass but an increase in LD size after CCTα silencing.

To assess the role of CCTα expression and de novo PC synthesis in adipocyte differentiation, we silenced CCTα in 3T3-L1 cells to prevent the twofold increase in PC synthesis during differentiation and maintain a biosynthetic rate similar to nondifferentiated cells (Figure 5B). Clearly, this basal level of PC synthesis was sufficient for differentiation, since we observed no decrease in the expression of PPARγ and adiponectin, and TAG mass was unaffected. However, suppressing PC synthesis reduced the number and increased the size of LDs in 3T3-L1 cells. This confirmed that the CDP-choline pathway provides PC for the surface monolayer that acts as a surfactant to prevent the coalescence of small LDs (Guo *et al.*, 2008). However, these results are at odds with a recent report showing that CCTα protein expression was not induced during differentiation of 3T3-L1 cells and CCTα silencing caused a reduction in perilipin expression and TAG deposition (Payne *et al.*, 2014). The reason for this discrepancy is not clear, since we observed an increase in CCTα expression using the commercial antibody described in that study (Supplemental Figure S1B), and the time course for expression of differentiation markers was similar. It is possible that inhibition of

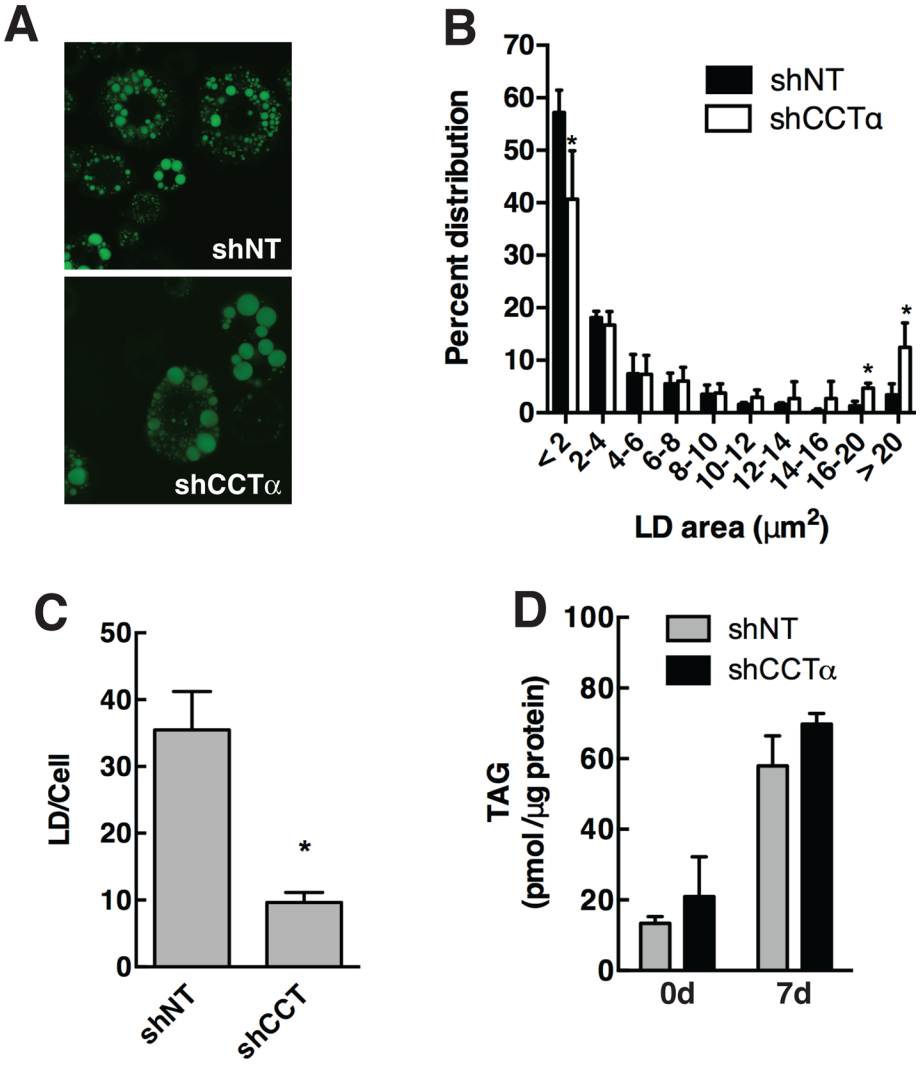

FIGURE 6: PC synthesis by the CDP-choline pathway regulates LD size in 3T3-L1 cells. (A) 3T3-L1 cells expressing shNT or shCCTα were either untreated or differentiated for 7 d, and LDs were visualized with BODIPY-493/503. (B) The size distribution of BODIPY-493/503 stained LDs in 7-d-differentiated control and knockdown cells was quantified using particle analysis features of ImageJ (version 1.48) and binned into area ranges. Results are the mean and SD of three or four fields of cells from three separate experiments. *$p < 0.05$ compared with matched shNT controls. (C) The total number of LDs in each cell was quantified from data in B. *$p < 0.05$ compared with matched shNT controls. (D) TAG mass was quantified in control and undifferentiated cells using an enzymatic assay. Results are the mean and SD of three experiments.

3T3-L1 differentiation observed by Payne *et al.* (2014) after CCTα silencing could be related to the lack of CCTα induction, which could result in a more profound suppression of PC synthesis and inhibition of TAG storage.

We also determined whether de novo PC synthesis is required for oleate-stimulated LD biogenesis in nonadipocytes. In this model, exogenous oleate supplied over a 24-h period is taken up by cells, esterified, and stored as TAG in cytoplasmic LDs. Oleate potently activates CCTα by promoting its dephosphorylation and translocation to membranes but does not increase CCTα expression (Pelech *et al.*, 1983; Cornell and Vance, 1987; Wang *et al.*, 1993). After screening a variety of cultured cells, we further characterized a nonmalignant IEC-18 that expressed nuclear CCTα and produced a large number of small LDs when challenged with oleate. Similar to 3T3-L1 cells, CCTα silencing in oleate-treated IEC-18 caused a reduction in LD number and increased LD size. However, TAG synthesis was also suppressed, and there was a significant loss of cell viability even at relatively low oleate concentrations. The inability of CCTα-deficient IEC-18 to synthesize and store TAG during acute induction of LD biogenesis supports a primary role for de novo PC synthesis in preventing fatty acid–induced toxicity. Without sufficient PC, primordial LD particles in the ER may not mature, thus limiting the capacity of the cell to synthesize and store TAG. 3T3-L1 cells in which the CDP-choline pathway is compromised would be buffered from fatty acid cytotoxicity due to induction of PEMT (Horl *et al.*, 2011) and expression of fatty acid–binding protein 4 (Hotamisligil *et al.*, 1996).

Treatment of cells with oleate results in the rapid (~5 min) translocation of endogenous and ectopically expressed CCTα to the inner nuclear envelope and nucleoplasmic reticulum before export into the cytoplasm (Lagace and Ridgway, 2005; Gehrig *et al.*, 2008b). Endogenous CCTα displayed a similar localization in differentiated 3T3-L1 cells and in some nonadipocyte cell lines after 12–24 h of oleate treatment. A striking feature of 3T3-L1 cells was the apparent translocation of nucleoplasmic CCTα to the nuclear envelope in cells containing large LDs. These cells also exhibited cytoplasmic CCTα, but at no time during differentiation was the enzyme detected on the surface of LDs. In human preadipocytes, CCTα was retained in the nucleus and did not appear on nuclear membranes during differentiation, perhaps reflecting a reduced requirement for PC during the biogenesis of large LDs with a low surface-to-volume ratio. In nonadipocyte cell lines treated with oleate to induce LD biogenesis, endogenous CCTα was activated on the nuclear envelope or appeared in the cytoplasm on small punctate structures that were interspersed with LDs but did not form discrete "rings" indicative of surface association. Similarly, epitope-tagged CCT was in the nucleus or nuclear envelope but not on the surface of LDs. FLIP experiments indicted that oleate treatment had no effect on the relatively slow exchange of CCT-GFP between the nuclear and cytoplasmic compartments, but association with the nuclear envelope was enhanced.

Our results are in stark contrast to the almost exclusive association of insect and mammalian CCTs with the surface of LDs in oleate-treated insect cells and the rapid (<30 s) shuttling of CCT1 between the nucleus and cytoplasm (Krahmer *et al.*, 2011; Payne *et al.*, 2014). The different phospholipid composition of insect and mammalian LDs likely accounts for this discrepancy. The PE/PC ratio in membranes and LDs from *Drosophila* S2 cell is ~3:1, whereas in mammalian LDs and membranes, the ratio is reversed (Jones *et al.*, 1992; Tauchi-Sato *et al.*, 2002; Krahmer *et al.*, 2011). The high content of PE, reduced PC, and presence of lipid activators such as oleate and

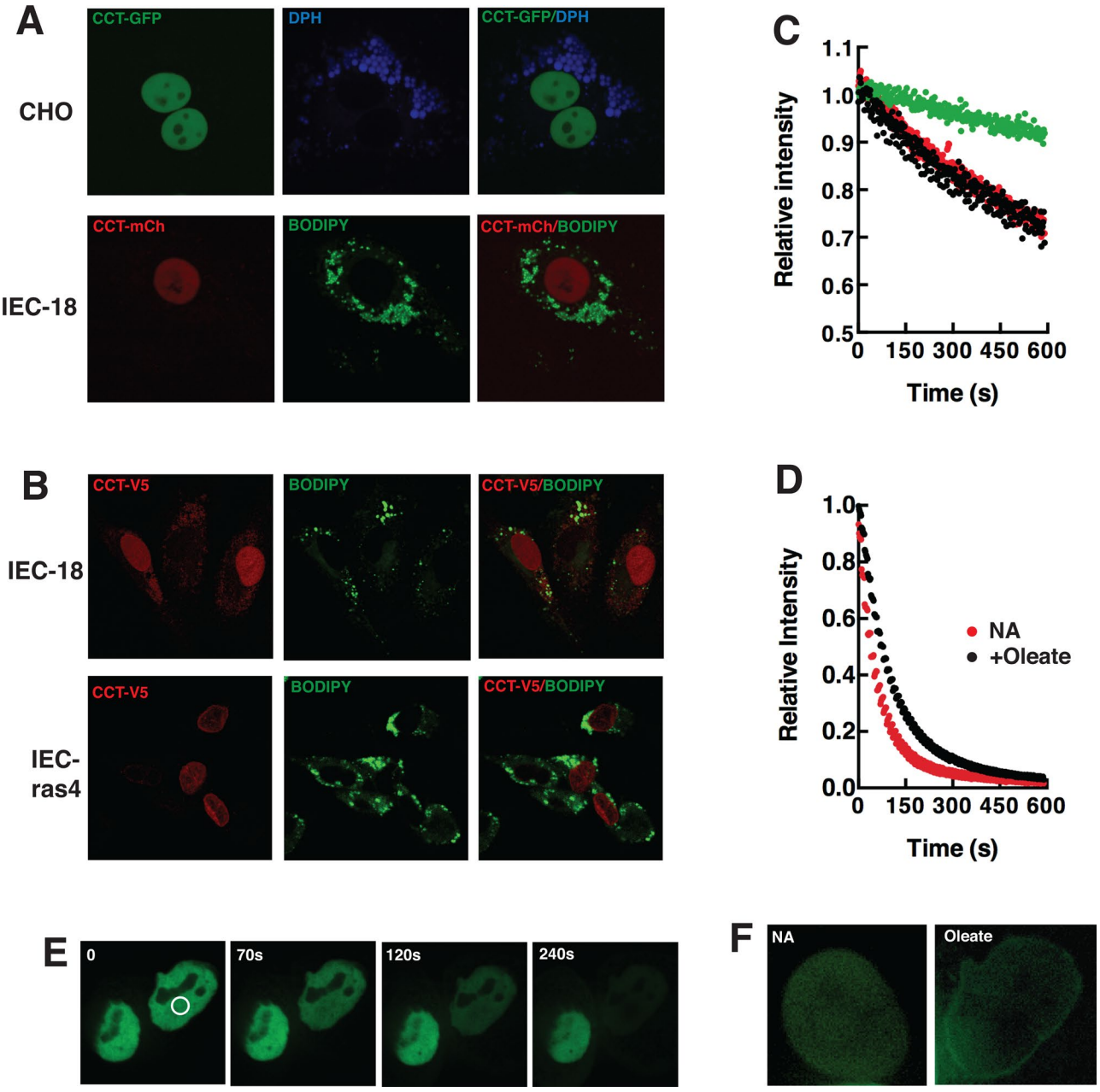

FIGURE 7: Localization of epitope-tagged CCTα in oleate-treated cells. (A) CHO and IEC-18 cells transiently expressing CCT-GFP or CCT-mCherry (CCT-mCh), respectively, were incubated with 400 μM oleate/BSA for 24 h. LDs were visualized by incubation with DPH or BODIPY-493/503. Spinning disk confocal images (1-μm sections) of live cells were captured as described in *Materials and Methods*. (B) IEC-18 and IEC-ras4 transiently expressing V5-tagged CCTα were treated with 400 μM oleate/BSA for 12 h before fixing and immunostaining with a V5-monoclonal and Alexa Fluor 594–conjugated secondary antibody. Images are 1-μm confocal sections captured using a Zeiss LSM510 META confocal microscope. (C) FLIP experiments in which the cytoplasm of CHO cells was repeatedly photobleached and relative fluorescence intensity of nuclear regions of interest (ROIs) were quantified. Green symbol, nonbleached cell; red symbol, no addition (NA); black symbol, oleate treated, 24 h. (D) FLIP experiment in which CHO cell nucleoplasm was repeatedly photobleached and the relative fluorescence intensity measured in a nuclear ROI. Results in C and D are the mean of four to nine cells from two separate experiments (error bars are removed for clarity). (E) FLIP analysis of an oleate-treated CHO cell (white circle indicates the photobleach area). (F) Nuclei of a control (NA) and oleate-treated CHO cell after the 10-min FLIP analysis shown in D. Image contrast and intensity was increased to visualize nuclear CCT-GFP.

DAG on the surface of *Drosophila* LDs would make this an optimal binding site for domain M in CCTα. On the basis of our inability to detect endogenous or overexpressed CCTα on LDs, we infer that this unique phospholipid lipid environment does not exist on the surface of mammalian LDs. Instead, PC deficiency and/or increased levels of lipid activators in the nuclear envelope or ER during LD biogenesis promotes CCTα recruitment and activation of CDP-choline synthesis at these membranes. ER-localized CEPT would then use the CDP-choline, either directly or after transport from the nucleus, to make PC for incorporation into LDs (Gehrig and Ridgway, 2011).

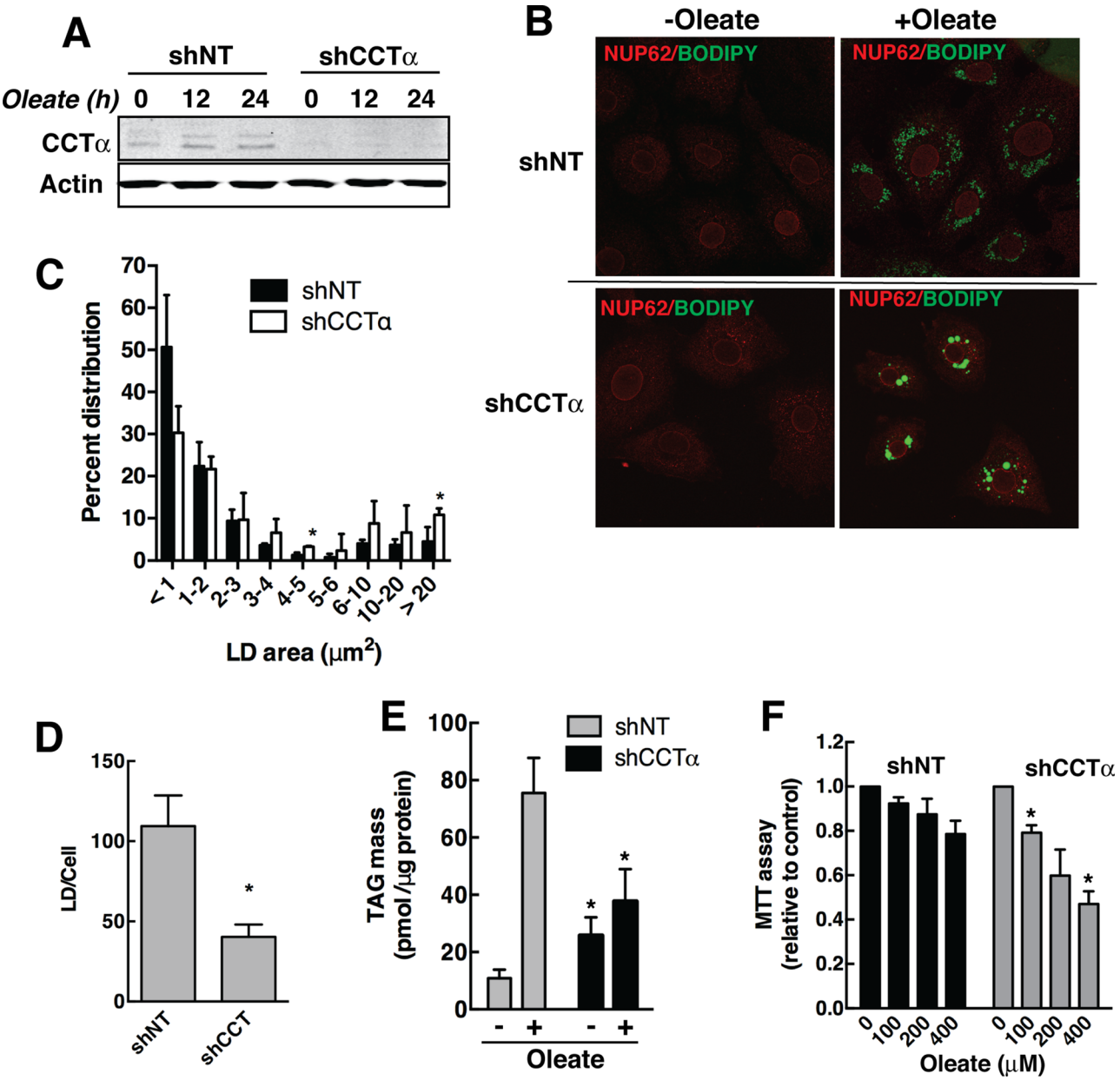

FIGURE 8: PC synthesis by the CDP-choline pathway regulates LD size and TAG mass in oleate-treated IEC-18 cells. (A) IEC-18 cells were stably transduced with lentivirus encoding shNT or shCCTα and treated with or without 400 μM oleate/BSA for up to 24 h. Cell lysates were immunoblotted for CCTα to confirm silencing. (B) shNT- and shCCTα-transduced IEC-18 cells treated with or without 400 μM oleate/BSA for 24 h were immunostained with the nuclear pore protein NUP62 antibody and an Alexa Fluor 594 secondary antibody. LDs were visualized with BODIPY-493/503. (C, D) The size distribution and number of LDs in IEC-18 cells stimulated with oleate for 24 h was quantified as described in the legend to Figure 6. *$p < 0.05$ compared with matched shNT. (E) TAG mass was quantified in oleate-treated IEC-18 cells expressing shNT and shCCTα cells using a colorimetric assay. Results are the mean and SD of three experiments. (F) The viability of shNT- and shCCTα-transduced IEC-18 treated with 0–400 μM oleate was measured using an MTT assay. Results are expressed relative to untreated cells and are the mean and SD of three experiments. *$p < 0.05$ compared with similarly treated shNT cells.

MATERIALS AND METHODS

Materials

Anti-adiponectin monoclonal antibody was purchased from Pierce-Thermo Fisher (Waltham, MA). PPARγ monoclonal antibody (E8) was from Santa Cruz Biotechnology (Dallas, TX). Anti-CCTα polyclonal antibody was raised in rabbits against a peptide from the C-terminal phosphorylation domain (GenScript, Scotch Plains, NJ). Anti-CCTα rabbit monoclonal antibody was purchased from Abcam (Toronto, Canada). Anti–choline kinase α antibody was from Proteintech Group (Chicago, IL). Anti-CCTβ antibody was provided by S. Jackowski (St. Jude Children's Research Hospital, Memphis, TN). TAG mass in cell lysates was quantified using a colorimetric assay according to the manufacturer's instructions (BioVision, Milpitas, CA). Cells lysates were solubilized in 0.1 ml of NP-40 (5% [wt/vol]), heated at 100°C for 5 min, and subjected to centrifugation at 10,000 × *g* for 2 min,

and the supernatant was diluted fivefold with water before the assay. Cell viability was assayed by measuring the reduction of MTT at 570 nm according to the manufacturer's instructions (Promega, Madison, WI). Oleate/BSA complexes (6:1 [mol/mol]) were sterilized by passage through a 0.45-μm filter (Goldstein, 1983).

Cell culture and adipocyte differentiation

All cells were maintained at 37°C in a humidified 5% CO_2 atmosphere. Intestinal epithelial cells (IEC-18) and an H-ras–transformed clone (IEC-ras4) were cultured in α-MEM supplemented with 5% fetal bovine serum (FBS), glucose (3.6 mg/ml), insulin (12.74 μg/ml), penicillin (600 μg/ml), streptomycin (100 μg/ml), and glutamine (2.92 mg/ml) (Rak *et al.*, 1995). CHO cells were cultured in DMEM supplemented with 5% FBS and proline (34 μg/ml). HEK293, HEK293T, 3T3-L1, and J774A cells were cultured in DMEM containing 10% FBS. HepG2 cells were cultured in the same medium supplemented with glutamine (2 mM).

Confluent cultures of 3T3-L1 preadipocytes were differentiated in DMEM containing 10% FBS and dexamethasone (1 μM), insulin (1 μg/ml), and isobutylmethylxanthine (IBMX, 0.5 mM) for 7 d (Kasturi and Wakil, 1983). Cryopreserved subcutaneous human preadipocytes were seeded at a density of 4×10^4 cell/cm^2 in preadipocyte media (DMEM/Ham's F-12 supplemented with 10% FBS, penicillin, streptomycin, and amphotericin B) until confluent (ZenBio, Research Triangle Park, NC). Cells were differentiated for 16 d in preadipocyte medium containing dexamethasone, insulin, IBMX, and rosiglitazone according to the manufacturer's instructions.

Lentivirus transduction and plasmid transfection

Lentivirus was produced in HEK293T cells by polyethyleneimine-mediated transfection of plasmids encoding a short hairpin RNA (shRNA; pLKO.1), packaging factors (pCMVΔ8.2), and vesicular stomatitis virus glycoprotein envelope protein (pCMV-VSVG). pLKO.1-shCCT encoded a CCTα-specific shRNA (CCTAAGGACATCTACAAGAA), and pLKO.1-shNT encoded a nontargeting control (CAACAAGATGAAGAGCACCAA; Arsenault *et al.*, 2013). After 72 h, virus-containing medium was collected, filtered, and supplemented with Polybrene (5 μg/ml). 3T3-L1 preadipocytes or IEC-18 were incubated with virus-containing media for 24 h and subsequently selected for 48–72 h in medium containing puromycin (1 μg/ml). The efficiency of CCTα silencing was determined by immunoblotting.

IEC-18 and CHO cells were transfected with pCCTα-GFP, pCCTα-mCherry, or pcDNA-CCT-V5/His (Lagace and Ridgway, 2005; Gehrig *et al.*, 2008a) using Lipofectamine 2000 according to manufacturer's instructions (Life Technologies, Burlington, Canada). Live- or fixed-cell fluorescence microscopy was performed 24 h after transfection.

Metabolic labeling with [^{3}H]choline

For time-course experiments, 3T3-L1 cells were differentiated at staggered intervals such that [^{3}H]choline labeling was done at the same time. Owing to the length of the differentiation period, human preadipocytes were cultured in differentiation medium at the same time, and [^{3}H]choline incorporation was measured at intervals up to 16 d. Human and 3T3-L1 adipocytes were cultured in their respective choline-free growth media and pulse-labeled with [^{3}H]choline (2 μCi/ml) for 3 h. Cells were rinsed once with cold phosphate-buffered saline (PBS) and harvested in methanol/water (2:1 [vol/vol]). [^{3}H]choline-labeled PC and water-soluble metabolites of the CDP-choline pathway (choline, phosphocholine, CDP-choline, and glycerophosphocholine) were extracted and resolved by thin-layer chromatography (TLC), and radioactivity in TLC scrapings was quantified by liquid scintillation counting (Storey *et al.*, 1997).

Immunostaining and microscopy

Cells cultured on glass coverslips were fixed with paraformaldehyde (4% [wt/vol]) in PBS for 15 min and then permeabilized in PBS containing BSA (1% [wt/vol]) and saponin (0.05% [wt/vol]). Coverslips were incubated sequentially in PBS containing BSA/saponin with primary antibodies and secondary antibodies conjugated with Alexa Fluor 488 or 594. LDs were visualized with BODIPY 493/503 or 1,6-diphenylhexatriene (DPH) added during the final secondary antibody incubation. Coverslips were mounted on glass slides with Mowiol 4-88, and images were captured using a Zeiss LSM510 META confocal microscope equipped with a 100×/numerical aperture (NA) 1.4 oil immersion objective (Zeiss, Jena, Germany). Lipid droplet size distribution was quantified using ImageJ software, version 1.47 (National Institutes of Health, Bethesda, MD). Briefly, images (three or four per experiment) were converted to 8-bit, the threshold was adjusted accordingly, and the "analyze particle" command was used to exclude on edges. Particle size distribution was 20 pixels^2 (lower cutoff) to infinity. The area distribution files were imported into Excel (Microsoft, Redmond, WA) and binned. Images of CCTα and LDs in human preadipocytes and mature adipocytes were captured using a Zeiss Axiovert 300M fluorescence microscope equipped with an AxioCam HRm charge-coupled device (CCD) and a 100×/NA 1.4 oil immersion objective.

CHO cells expressing CCT-GFP and treated with oleate (400 mM)/BSA were incubated with DPH for 15 min before live-cell imaging. Oleate-treated IEC-18 expressing CCT-mCherry were incubated with BODIPY 493/503 for 15 min before imaging. Images of live cells were captured using a Zeiss Cell Observer microscope equipped with a CSU-X1 confocal scanner (Yokogawa, Tokyo, Japan), an AxioCam HRm CCD, and a Plan-Apochromat 63×/1.40 NA oil immersion objective.

For FLIP experiments, CHO cells expressing CCT-GFP were treated with or without oleate (400 mM)/BSA for 24 h. A cytosolic or nuclear target (4-μm diameter) was bleached for 250 ms at 10-s intervals (80% maximum intensity, 488-nm laser). Images were acquired at 2-s intervals using the described spinning disk confocal microscope and an Evolve CCD (Photometrics, Tucson, AZ). The fluorescence intensity of nuclear regions of interest (which did not include the nuclear envelope) was quantified using Zeiss Zen 2012 Blue software (version 1.1.2.0).

ACKNOWLEDGMENTS

We thank Robert Douglas and Mark Charman for excellent technical assistance. This work was supported by an operating grant from the Canadian Institutes of Health Research (MOP-136809).

REFERENCES

Agassandian M, Chen BB, Pulijala R, Kaercher L, Glasser JR, Mallampalli RK (2012). Calcium-calmodulin kinase I cooperatively regulates nucleocytoplasmic shuttling of CCTalpha by accessing a nuclear export signal. Mol Biol Cell 23, 2755–2769.

Agassandian M, Chen BB, Schuster CC, Houtman JC, Mallampalli RK (2010). 14-3-3zeta escorts CCTalpha for calcium-activated nuclear import in lung epithelia. FASEB J 24, 1271–1283.

Arnold RS, Cornell RB (1996). Lipid regulation of CTP: phosphocholine cytidylyltransferase: electrostatic, hydrophobic, and synergistic interactions of anionic phospholipids and diacylglycerol. Biochemistry 35, 9917–9924.

Arsenault DJ, Yoo BH, Rosen KV, Ridgway ND (2013). ras-Induced up-regulation of CTP:phosphocholine cytidylyltransferase alpha contributes to malignant transformation of intestinal epithelial cells. J Biol Chem 288, 633–643.

Bartz R, Li WH, Venables B, Zehmer JK, Roth MR, Welti R, Anderson RG, Liu P, Chapman KD (2007). Lipidomics reveals that adiposomes store ether lipids and mediate phospholipid traffic. J Lipid Res 48, 837–847.

Chen BB, Mallampalli RK (2009). Masking of a nuclear signal motif by monoubiquitination leads to mislocalization and degradation of the regulatory enzyme cytidylyltransferase. Mol Cell Biol 29, 3062–3075.

Coleman RA, Reed BC, Mackall JC, Student AK, Lane MD, Bell RM (1978). Selective changes in microsomal enzymes of triacylglycerol phosphatidylcholine, and phosphatidylethanolamine biosynthesis during differentiation of 3T3-L1 preadipocytes. J Biol Chem 253, 7256–7261.

Cornell RB, Northwood IC (2000). Regulation of CTP:phosphocholine cytidylyltransferase by amphitropism and relocalization. Trends Biochem Sci 25, 441–447.

Cornell R, Vance DE (1987). Translocation of CTP: phosphocholine cytidylyltransferase from cytosol to membranes in HeLa cells: stimulation by fatty acid, fatty alcohol, mono- and diacylglycerol. Biochim Biophys Acta 919, 26–36.

Fagone P, Jackowski S (2012). Phosphatidylcholine and the CDP-choline cycle. Biochim Biophys Acta 1831, 523–532.

Gehrig K, Cornell RB, Ridgway ND (2008a). Expansion of the nucleoplasmic reticulum requires the coordinated activity of lamins and CTP:phosphocholine cytidylyltransferase alpha. Mol Biol Cell 19, 237–247.

Gehrig K, Morton CC, Ridgway ND (2008b). Nuclear export of the rate-limiting enzyme in phosphatidylcholine synthesis is mediated by its membrane binding domain. J Lipid Res 50, 966–976.

Gehrig K, Ridgway ND (2011). CTP:phosphocholine cytidylyltransferase alpha (CCTalpha) and lamins alter nuclear membrane structure without affecting phosphatidylcholine synthesis. Biochim Biophys Acta 1811, 377–385.

Goldstein JL, Basu SK, Brown MS (1983). Receptor mediated endocytosis of low-density lipoprotein in cultured cells. Methods Enzymol 98, 241–260.

Guo Y, Walther TC, Rao M, Stuurman N, Goshima G, Terayama K, Wong JS, Vale RD, Walter P, Farese RV (2008). Functional genomic screen reveals genes involved in lipid-droplet formation and utilization. Nature 453, 657–661.

Henneberry AL, Wistow G, McMaster CR (2000). Cloning, genomic organization, and characterization of a human cholinephosphotransferase. J Biol Chem 275, 29808–29815.

Henneberry AL, Wright MM, McMaster CR (2002). The major sites of cellular phospholipid synthesis and molecular determinants of fatty acid and lipid head group specificity. Mol Biol Cell 13, 3148–3161.

Horl G, Wagner A, Cole LK, Malli R, Reicher H, Kotzbeck P, Kofeler H, Hofler G, Frank S, Bogner-Strauss JG, *et al.* (2011). Sequential synthesis and methylation of phosphatidylethanolamine promote lipid droplet biosynthesis and stability in tissue culture and in vivo. J Biol Chem 286, 17338–17350.

Hotamisligil GS, Johnson RS, Distel RJ, Ellis R, Papaioannou VE, Spiegelman BM (1996). Uncoupling of obesity from insulin resistance through a targeted mutation in aP2, the adipocyte fatty acid binding protein. Science 274, 1377–1379.

Jones HE, Harwood JL, Bowen ID, Griffiths G (1992). Lipid composition of subcellular membranes from larvae and prepupae of Drosophila melanogaster. Lipids 27, 984–987.

Kassan A, Herms A, Fernandez-Vidal A, Bosch M, Schieber NL, Reddy BJ, Fajardo A, Gelabert-Baldrich M, Tebar F, Enrich C, *et al.* (2013). Acyl-CoA synthetase 3 promotes lipid droplet biogenesis in ER microdomains. J Cell Biol 203, 985–1001.

Kast HR, Nguyen CM, Anisfeld AM, Ericsson J, Edwards PA (2001). CTP:phosphocholine cytidylyltransferase, a new sterol- and SREBP-responsive gene. J Lipid Res 42, 1266–1272.

Kasturi R, Wakil SJ (1983). Increased synthesis and accumulation of phospholipids during differentiation of 3T3-L1 cells into adipocytes. J Biol Chem 258, 3559–3564.

Krahmer N, Farese RV Jr, Walther TC (2013). Balancing the fat: lipid droplets and human disease. EMBO Mol Med 5, 905–915.

Krahmer N, Guo Y, Wilfling F, Hilger M, Lingrell S, Heger K, Newman HW, Schmidt-Supprian M, Vance DE, Mann M, *et al.* (2011). Phosphatidylcholine synthesis for lipid droplet expansion is mediated by localized activation of CTP:phosphocholine cytidylyltransferase. Cell Metab 14, 504–515.

Lagace TA, Ridgway ND (2005). The rate-limiting enzyme in phosphatidylcholine synthesis regulates proliferation of the nucleoplasmic reticulum. Mol Biol Cell 16, 1120–1130.

Lykidis A, Murti KG, Jackowski S (1998). Cloning and characterization of a second human CTP:phosphocholine cytidylyltransferase. J Biol Chem 273, 14022–14029.

Moessinger C, Klizaite K, Steinhagen A, Philippou-Massier J, Shevchenko A, Hoch M, Ejsing CS, Thiele C (2014). Two different pathways of phosphatidylcholine synthesis, the Kennedy Pathway and the Lands Cycle, differentially regulate cellular triacylglycerol storage. BMC Cell Biol 15, 43–51.

Moessinger C, Kuerschner L, Spandl J, Shevchenko A, Thiele C (2011). Human lysophosphatidylcholine acyltransferases 1 and 2 are located in lipid droplets where they catalyze the formation of phosphatidylcholine. J Biol Chem 286, 21330–21339.

Payne F, Lim K, Girousse A, Brown RJ, Kory N, Robbins A, Xue Y, Sleigh A, Cochran E, Adams C, *et al.* (2014). Mutations disrupting the Kennedy phosphatidylcholine pathway in humans with congenital lipodystrophy and fatty liver disease. Proc Natl Acad Sci USA 111, 8901–8906.

Pelech SL, Pritchard PH, Brindley DN, Vance DE (1983). Fatty acids promote translocation of CTP:phosphocholine cytidylyltransferase to the endoplasmic reticulum and stimulate rat hepatic phosphatidylcholine synthesis. J Biol Chem 258, 6782–6788.

Pol A, Gross SP, Parton RG (2014). Review: biogenesis of the multifunctional lipid droplet: lipids, proteins, and sites. J Cell Biol 20, 635–646.

Rak J, Mitsuhashi Y, Erdos V, Huang SN, Filmus J, Kerbel RS (1995). Massive programmed cell death in intestinal epithelial cells induced by three-dimensional growth conditions: suppression by mutant c-H-ras oncogene expression. J Cell Biol 131, 1587–1598.

Ridgway ND, Vance DE (1988). Specificity of rat hepatic phosphatidylethanolamine N-methyltransferase for molecular species of diacyl phosphatidylethanolamine. J Biol Chem 263, 16856–16863.

Shields DJ, Lehner R, Agellon LB, Vance DE (2003). Membrane topography of human phosphatidylethanolamine N-methyltransferase. J Biol Chem 278, 2956–2962.

Storey MK, Byers DM, Cook HW, Ridgway ND (1997). Decreased phosphatidylcholine biosynthesis and abnormal distribution of CTP:phosphocholine cytidylyltransferase in cholesterol auxotrophic Chinese hamster ovary cells. J Lipid Res 38, 711–722.

Tauchi-Sato K, Ozeki S, Houjou T, Taguchi R, Fujimoto T (2002). The surface of lipid droplets is a phospholipid monolayer with a unique fatty acid composition. J Biol Chem 277, 44507–44512.

Wang Y, MacDonald JI, Kent C (1993). Regulation of CTP:phosphocholine cytidylyltransferase in HeLa cells. Effect of oleate on phosphorylation and intracellular localization. J Biol Chem 268, 5512–5518.

Watkins JD, Kent C (1992). Immunolocalization of membrane-associated CTP:phosphocholine cytidylyltransferase in phosphatidylcholine-deficient Chinese hamster ovary cells. J Biol Chem 267, 5686–5692.

Yang W, Boggs KP, Jackowski S (1995). The association of lipid activators with the amphipathic helical domain of CTP:phosphocholine cytidylyltransferase accelerates catalysis by increasing the affinity of the enzyme for CTP. J Biol Chem 270, 23951–23957.